HHS Public Access

Author manuscript

Nat Neurosci. Author manuscript; available in PMC 2017 March 26.

Published in final edited form as:

Nat Neurosci. 2016 November ; 19(11): 1506–1512. doi:10.1038/nn.4395.

MeCP2 and Histone Deacetylases 1 and 2 in Dorsal Striatum Collectively Suppress Repetitive Behaviors

Melissa Mahgoub[1], **Megumi Adachi**[1], **Kanzo Suzuki**[1], **Xihui Liu**[1], **Ege T. Kavalali**[1,2], **Maria H. Chahrour**[1,3], and **Lisa M. Monteggia**[1]

[1]Department of Neuroscience, UT Southwestern Medical Center, Dallas, Texas 75390, USA

[2]Department of Physiology, UT Southwestern Medical Center, Dallas, Texas 75390, USA

[3]Eugene McDermott Center for Human Growth and Development, UT Southwestern Medical Center, Dallas, Texas 75390, USA

Abstract

Class I histone deacetylases (HDACs), HDAC1 and HDAC2 often associate together in protein complexes with transcriptional factors such as methyl-CpG-binding protein 2 (MeCP2). Given their high degree of sequence identity, we examined the functional redundancy of HDAC1 and HDAC2 in mature brain. We demonstrate that postnatal forebrain-specific deletion of both *HDAC1* and *HDAC2* in mice impacts neuronal survival and results in an excessive grooming phenotype caused by dysregulation of the obsessive-compulsive disorder-implicated gene SAP90/PSD-95-associated protein 3 (*SAPAP3*) in striatum. Moreover, HDAC1- and HDAC2-dependent regulation of SAPAP3 expression requires *Mecp2*, the gene involved in the pathophysiology of Rett syndrome. We show that postnatal forebrain-specific deletion of *Mecp2* causes excessive grooming, which is rescued by restoring striatal *Sapap3* expression. Our results provide novel insight into the upstream regulation of *SAPAP3*, and establish the essential role of striatal HDAC1, HDAC2, and MeCP2 for suppression of repetitive behaviors.

Keywords

MeCP2; behavior; grooming; obsessive-compulsive disorder; Sapap3

Correspondence: Lisa M. Monteggia, Department of Neuroscience, University of Texas Southwestern Medical Center, 5323 Harry Hines Blvd, Dallas, TX 75390-9111, Tel: 214-648-5548, lisa.monteggia@utsouthwestern.edu.

Competing financial interests

L. Monteggia is on the scientific advisory board for Rodin Therapeutics.

Author Contributions

M. Mahgoub and M. Adachi performed the behavioral experiments. M. Mahgoub, M. Adachi, K. Suzuki, M. Chahrour, and X. Liu, contributed to the molecular experiments. M. Mahgoub performed the statistical analyses. M. Mahgoub made the figures and wrote the corresponding sections of the paper. L. Monteggia and E. Kavalali designed the study, supervised the experiments and wrote the paper.

Data availability

The data that support the findings of this study are available from the corresponding author upon request.

Introduction

Histone deacetylases (HDACs) are a class of enzymes that remove acetyl groups from histone tails and promote chromatin remodeling[1]. The role of individual HDACs in the brain is an active area of investigation with recent data suggesting that the Class I HDAC, HDAC2, is a negative regulator of learning and memory[2–6]. HDAC2 shares 85% sequence identity with another Class I family member, HDAC1, however loss of HDAC1 in the brain does not impact learning and memory[7,8]. The target genes of HDAC1 and HDAC2 in brain are unclear and distinguishing their functional roles is complicated by the fact that HDAC1 and HDAC2 can also associate to form a complex with other proteins, such as Methyl-CpG binding protein 2 (MeCP2) to regulate gene expression[1,9–11].

MeCP2 is a transcription factor known to play important roles in mediating complex behavior and synaptic function[12–16]. Loss of function mutations in *MECP2* lead to the neurological disorder Rett syndrome[17] (RTT), and genomic duplications spanning *MECP2* also result in neurological abnormalities with autistic features and behaviors[18]. RTT patients display a range of phenotypes including repetitive behaviors such as stereotypical hand movements, similar to phenotypes observed in patients with obsessive-compulsive disorder (OCD)[19,20]. Previous studies have shown that mice lacking MeCP2 recapitulate several of the behavioral aspects of RTT, including social and motor deficits[12–14,21,22].

In the present study we were interested in examining whether postnatal deletion of both HDAC1 and HDAC2 results in the phenotypes observed in mice with a brain specific deletion of HDAC2. Rather surprisingly, we identified a functional redundancy between HDAC1 and HDAC2 in neuronal survival that impacted the lifespan of the *HDAC1/HDAC2* double knockout mice. We also observed exacerbated grooming behavior that was due to dysregulation of SAPAP3 in the striatum, with a similar phenotype to conditional *Mecp2* knockout mice. We were able to rescue the grooming phenotype in conditional *Mecp2* knockout mice by expression of SAPAP3 in the striatum suggesting that *SAPAP3* is a putative target gene of MeCP2 in association with HDAC1 and HDAC2. Collectively, our data reveal unexpected negative effects of HDAC inhibition in postnatal brain as well as uncover the role of HDAC1, HDAC2, and MeCP2 in regulation of *SAPAP3*, a gene linked to obsessive-compulsive disorder (OCD).

Results

Postnatal loss of *HDAC1* and *HDAC2* results in behavioral abnormalities and premature death

To examine the role of HDAC1 and HDAC2 in mature brain, we generated mice with forebrain specific deletions of both genes during postnatal development. Homozygous $HDAC1^{loxP/loxP}/HDAC2^{loxP/loxP}$ mice[23] were crossed to calcium/calmodulin-dependent protein kinase II *(CaMKII)-Cre93* mice to generate the conditional deletion of *Hdac1* and *Hdac2* (referred to as cDKO) in forebrain regions during postnatal development[13]. To determine whether potential phenotypes were due to the loss of both *HDAC1* and *HDAC2* and not the result of the deletion of either individual HDAC, conditional *HDAC1* knockout (*HDAC1* cKO) mice as well as conditional *HDAC2* knockout (*HDAC2* cKO) mice were

generated using *CaMKII-Cre93*. The cDKO mice were born at normal Mendelian ratios and appeared indistinguishable from littermate controls (CTLs) at birth. Immunohistochemistry and western blot analysis of the cDKO mice at 8 weeks of age confirmed the deletion of HDAC1 and HDAC2 in forebrain regions including frontal cortex, hippocampus and striatum with no change in expression in cerebellum (Fig. 1 a–d), consistent with the original characterization of the *CaMKII-Cre93* line[13]. Individual *HDAC1* cKO or *HDAC2* cKO mice showed a similar pattern of deletion of the gene of interest[8]. The cDKO mice were indistinguishable in body weight from littermate CTLs for the first few weeks of life, however, at 6 weeks of age the cDKO mice began to lose weight (Fig. 2a) and all cDKO mice died at ~9 weeks of age. Mice with a single copy of either allele did not show alterations in weight nor early postnatal lethality (data not shown). The *HDAC1* cKO or *HDAC2* cKO mice were also indistinguishable from littermate CTLs in weight and had a normal lifespan (Supplementary Fig. 1a,b). Collectively, these data are consistent with loss of both HDAC1 and HDAC2 in postnatal forebrain regions impacting the viability of the mice.

Necroscopic analysis of cDKO mice did not reveal peripheral abnormalities (data not shown). However, there was a significant reduction in overall brain size and weight in 8 week old cDKO mice compared to age matched CTLs, which appeared to be due to a decrease in the size of the cortical areas, consistent with the regional deletion of *HDAC1* and *HDAC2* (Fig. 2b, Supplementary Fig. 1e). The *CaMKII-Cre93* line expresses Cre recombinase at postnatal days 10–14, therefore we examined the brain mass of cDKO mice at a time point coinciding with early expression of Cre recombinase[13], postnatal day 16, and found no difference compared to CTLs (Fig. 2c), demonstrating that the reduction in brain size occurred after the deletion of *HDAC1* and *HDAC2*. We also observed no differences in brain weight in 8 week old *HDAC1* cKO or *HDAC2* cKO mice, further supporting that deletion of both *HDAC1* and *HDAC2* led to the reduction in brain mass (Supplementary Fig. 1c,d). Hematoxylin and eosin (H&E) staining revealed aberrant cellular patterns and layering in cortex (Fig. 2e **and enlarged**) and hippocampus (Fig. 2i **and enlarged**) of cDKO mice compared to CTLs (Fig. 2d,h, **and enlarged**). Rather surprisingly, there were no cell morphology abnormalities observed in the striatum of cDKOs compared to CTLs (Fig. 2f,g) although HDAC1 and HDAC2 expression was significantly reduced in this brain region (Fig. 1a–d), as *CaMKII–Cre93* is known to express Cre recombinase in medium spiny neurons of the striatum[24]. There were also no detectable differences in the cerebellar structure between cDKO and CTL mice, consistent with the forebrain specific deletion (Fig. 2j,k). Terminal deoxynucleotidyl transferase dUTP nick end labeling (TUNEL) revealed increased apoptosis in the cortex and hippocampus, but not in the striatum or cerebellum of cDKOs compared to CTLs consistent with the regional morphological changes (Supplementary Fig. 2), demonstrating a functional redundancy of HDAC1 and HDAC2 on cell survival in cortex and hippocampus.

We examined whether 6 week old cDKO mice, at the time of onset for weight loss, had alterations in locomotor activity or anxiety related behavior. The cDKO mice were significantly hypoactive (Supplementary Fig. 3d **and inset**) and spent less time in the center of the arena and more time in the periphery in the open field test, suggestive of an increase

in anxiety-like behavior (Supplementary Fig. 3e). We also assessed these behaviors in a separate cohort of 3 week old mice, a time point ~1 week after the expression of Cre recombinase, and found that cDKO mice were significantly hypoactive (Supplementary Fig. 3a **and inset**) with heightened anxiety-related behavior (Supplementary Fig. 3b), showing that loss of both HDAC1 and HDAC2 rapidly contributed to this phenotype.

HDAC1/HDAC2 cDKO mice develop a facial lesion and display excessive grooming similar to OCD-like behaviors

We observed that every cDKO mouse developed a severe lesion on the face and neck regions at ~7 weeks of age (Fig. 3a). The fur lesion could not be attributed to fighting with cage mates as the lesion still appeared in each cDKO mice that was singly housed after weaning (3 weeks of age prior to the appearance of the fur lesion; data not shown), and not in any CTL or *HDAC1/2* double heterozygous cage mates, suggesting the lesions were not the result of allogrooming. We also did not observe facial or neck lesions on any of the *HDAC1* cKO or *HDAC2* cKO mice, demonstrating that the lesion was the result of loss of both *HDAC1* and *HDAC2*. The lesion did not appear to be due to any form of dermatitis, therefore we investigated whether the fur lesion was due to excessive grooming in cDKO mice. We monitored the behavior of 3 and 6 week old cDKO mice for a 30 minute time period (between 8 am – 12 pm) and scored the total amount of time the mouse spent self-grooming. As most studies only score the initial 10 minute period, we assessed this time interval and found the cDKO mice spent approximately twice the amount of time grooming as CTL mice (Fig. 3b; Supplementary Fig. 3c). The phenotype was consistent at the 20 minute, as well as the 30 minute time interval, revealing a significant more than two-fold increase in grooming of cDKO mice compared to CTLs. In contrast, *HDAC1* cKO or *HDAC2* cKO mice show normal grooming behavior compared to their respective littermate CTLs (Supplementary Fig. 4a,b), demonstrating that the fur lesion as well as the excessive grooming phenotype is due to concurrent loss of *HDAC1* and *HDAC2*.

Chronic administration of fluoxetine attenuates excessive grooming

Increased grooming in mice has been suggested to model aspects of obsessive-compulsive disorder (OCD), with previous data establishing that the serotonin selective reuptake inhibitor (SSRI), fluoxetine, can alleviate excessive grooming in mice[25,26] similar to the attenuation of symptoms in individuals with OCD[27–29]. We treated 3 week old cDKO and littermate CTLs with fluoxetine (intraperitoneal injections, 10 mg kg^{-1}/day) and examined whether the excessive grooming behavior in cDKO mice was responsive to the drug treatment. We found that one week of fluoxetine treatment did not attenuate the increased grooming behavior of the cDKO mice (Supplementary Fig. 4c). However, three weeks of fluoxetine administration significantly reduced the amount of time spent grooming comparable to a level seen in CTLs (Fig. 3c), recapitulating clinical data that SSRIs take several weeks to reach efficacy[30].

HDAC1/HDAC2 cDKO mice have altered *Sapap3* expression

The gene encoding post-synaptic scaffolding protein SAP90/PSD-95-associated protein 3 (SAPAP3) is linked to obsessive-compulsive and grooming disorders in humans[31,32]. Mice

lacking *Sapap3* display an excessive grooming phenotype resulting in a facial lesion[25], similar to the cDKO mice. We therefore assessed whether *Sapap3* expression was altered by the loss of *HDAC1* and *HDAC2*. Quantitative-RT (qRT) PCR analysis revealed a significant decrease in *Sapap3* expression in frontal cortex and striatum, with no alterations in hippocampus and cerebellum (Fig. 3d), in cDKO mice. This result is in agreement with previous work showing that the grooming phenotype of the *Sapap3* knockout mice is mediated through the corticostriatal pathway[25]. *Sapap3* expression was not altered in *HDAC1* cKO or *HDAC2* cKO mice consistent with the premise that loss of both *HDAC1* and *HDAC2* was necessary to dysregulate its expression (Supplementary Fig. 4d,e). We also examined the expression of *Slitrk5*, another gene that has been linked to excessive grooming behavior in mice[26], and found no change in expression in the striatum or cortex, showing specificity for the altered *Sapap3* expression in the cDKO mice (Supplementary Fig. 4f).

Striatal specific deletion of *HDAC1/HDAC2* recapitulates excessive grooming seen in cDKO mice

We next examined whether deletion of *HDAC1* and *HDAC2* selectively in the striatum is sufficient to disrupt *Sapap3* expression and elicit the excessive grooming behavior. We used stereotaxic methods to bilaterally inject into the dorsal striatum of adult $Hdac1^{loxP/loxP}/Hdac2^{loxP/loxP}$ mice an adeno-associated viral (AAV) vector expressing Green Fluorescent Protein tagged to Cre recombinase (GFP-Cre) or GFP alone as a control (Fig. 4a). Mice were behaviorally tested three weeks after surgery, a time point sufficient for Cre mediated recombination with AAV-GFP-Cre[33] then sacrificed to confirm viral placements using laser microscopy (Fig. 4b), with off-target injected animals eliminated from further analysis. qRT-PCR showed an approximate 50% reduction in *HDAC1* and *HDAC2* expression in dorsal striatum of AAV-GFP-Cre compared to AAV-GFP injected mice (Fig. 4c). The striatum specific deletion of *HDAC1* and *HDAC2* did not result in any obvious structural alterations or cell death within the striatum (Supplemental Fig. 5d), and did not impact lifespan, weight, locomotor activity, anxiety-like behavior, or motor coordination compared to AAV-GFP injected mice (Supplementary Fig. 5a–c). However, deletion of *HDAC1* and *HDAC2* selectively in the striatum resulted in a significant increase in the time spent grooming (Fig. 4d) with a significant decrease in *Sapap3* expression in the striatum compared to AAV-GFP injected mice (Fig. 4e) similar to data from the cDKO mice.

Postnatal conditional deletion of *Mecp2* recapitulates OCD-like phenotype of cDKO mice

Our data so far demonstrate that loss of both *HDAC1* and *HDAC2* in the striatum down-regulates *Sapap3* expression and results in an excessive grooming phenotype. HDAC1 and HDAC2 do not bind DNA directly[1,9,34] but rather participate in protein complexes to impact gene transcription. Methyl-CpG-binding protein 2 (MeCP2) is a transcription factor that has been shown to interact with HDAC1 and HDAC2 in a co-repressor complex and regulate gene expression[10,11]. We confirmed that this interaction also occurs in the striatum by crossing $Mecp2^{2loxP/+}$ mice with *CaMKII-Cre93* mice to generate conditional *Mecp2* knockout mice (*Mecp2* cKO), and performing immunoprecipitation (IP) with an antibody against HDAC2 on striatal samples from CTL and *Mecp2* cKO mice (Supplementary Fig. 6). The function of MeCP2 in the central nervous system is complex, as it has been shown to activate and repress transcription[11,35,36]. To investigate whether MeCP2 binds the *Sapap3*

promoter, we performed chromatin immunoprecipitation (ChIP) from the striatum of MeCP2 cKO mice and CTLs using an antibody to MeCP2. QPCR analysis of the ChIP DNA revealed specific MeCP2 binding to the *Sapap3* promoter region (as indicated by the H3K4me3 promoter mark) ~600 bp upstream of the transcriptional start site (P600), adjacent to a CpG island (Fig. 5 a,b). HDACs are not known to bind DNA directly[1,9,34], suggesting that MeCP2 is mediating the effects of HDAC1 and HDAC2 on SAPAP3 function. Consistent with our results, previous work has shown that mice with loss of *Mecp2* in inhibitory forebrain neurons display an excessive grooming phenotype[22]. In our experiments, the *CaMKII-Cre93* line used to generate the *Mecp2* cKO mice expresses Cre recombinase in excitatory neurons in broad forebrain regions as well as inhibitory medium spiny neurons in the striatum[24]. We found that *Mecp2* cKO mice also show a significant increase in time spent grooming (Fig. 5c) with a significant decrease in *Sapap3* expression in the striatum (Fig. 5d) compared to littermate CTLs.

Restoring *Sapap3* in striatum of *Mecp2* cKO mice rescues excessive grooming phenotype

To establish a direct link between MeCP2 and SAPAP3 in mediating the grooming phenotype, we generated adeno-associated DJ serotype viruses expressing either GFP only (control) or an HA-tagged SAPAP3 (AAV-SAPAP3), and stereotaxically injected them bilaterally into the dorsal striatum of adult *Mecp2* cKO and CTL mice to test whether this would rescue the grooming phenotype (Fig. 6a). We confirmed the localized expression of SAPAP3 to the dorsal striatum by immunohistochemistry (Fig. 6b). We also corroborated the rescue of *Sapap3* expression in the striatum of *Mecp2* cKO mice injected with the AAV-SAPAP3 virus by qRT-PCR analysis (Fig. 6c). We found that AAV-mediated expression of SAPAP3 in the striatum of the *Mecp2* cKO mice rescued the excessive grooming behavior to a level comparable to CTL mice injected with GFP alone (Fig. 6d), indicating that this deficit was the result of decreased expression of *Sapap3*. The AAV expression of *Sapap3* in the dorsal striatum did not alter locomotor activity, and in contrast to the reversal of the grooming phenotype, the previously reported impaired performance of the *Mecp2* cKO mice on the rotarod[14] was still present (Supplemental Fig. 7a,b), suggesting this deficit is mediated through a different mechanism.

Discussion

Our results reveal that postnatal deletion of both *HDAC1* and *HDAC2* in the brain results in several adverse effects, including neuronal apoptosis in cortical and hippocampal regions as well as early postnatal lethality, demonstrating functionally redundant roles in neuronal survival past embryogenesis. Given the recent efforts in the development of HDAC2 inhibitors for the treatment of neurodegeneration and cognitive enhancement, our results suggest caution with compounds targeting both HDAC1 and HDAC2, and emphasize the importance of subtype specific inhibitors. We also observed that the concurrent loss of *HDAC1* and *HDAC2* results in an increase in striatum-dependent repetitive behaviors and dysregulation of *Sapap3* expression, a gene linked to obsessive-compulsive and grooming disorders in humans[31,32]. We were able to demonstrate that the selective deletion of *HDAC1* and *HDAC2* in the dorsal striatum results in altered *Sapap3* expression as well as increased repetitive grooming similar to that observed in cDKO mice. *Mecp2*, the gene that causes

Rett syndrome and various neurodevelopmental abnormalities, has been shown to interact with HDAC1 and HDAC2 in a protein complex[14,15]. We find that MeCP2 binds to the *Sapap3* promoter and that deletion of *Mecp2* in broad forebrain regions of the mouse, similar to the loss of *Mecp2* in inhibitory neurons[22], results in increased repetitive behaviors as well as decreased *Sapap3* expression in the dorsal striatum. We then show that the grooming phenotype in the *Mecp2* cKO mice can be rescued by reintroducing *Sapap3* expression in the dorsal striatum. Our results showing that MeCP2 binds to the *Sapap3* promoter, that loss of *Mecp2* attenuates *Sapap3* expression, and that restoring *Sapap3* in the striatum rescues the grooming phenotype, suggests that the repetitive behaviors observed in Rett syndrome may be due to dysregulation of *SAPAP3* in the striatum. Collectively, these data suggest that HDAC1 and HDAC2 in concert with MeCP2 within the striatum regulate repetitive behaviors through transcription dependent processes, and provide novel insight into the neurobiological mechanisms underlying repetitive behaviors.

Methods Summary

Animals were housed and maintained as previously described[8]. Molecular studies consisted of western blot analysis, quantitative PCR, or chromatin immunoprecipitation on tissue lysates from frontal cortex, hippocampus, striatum, or cerebellum. Histological analysis consisted of immunohistochemistry, terminal deoxynucleotidyltransferase-mediated UTP end labeling, and Hematoxylin and Eosin staining and performed as previously described[8,38]. Behavioral studies and stereotaxic surgeries were performed using male mice as previously described[8,21]. Obsessive-compulsive-like behavior was assessed by scoring grooming behavior. Briefly, mice were placed in a home cage environment and total time spent grooming was measured for 30 minutes. All drugs were administered via intraperitoneal injection. All experiments were performed and analyzed blind to test variable. Sample sizes were estimated based on our previous experience performing similar experiments.

Mice

The conditional *Hdac1* knockout (*Hdac1* cKO), *Hdac2* knockout (*Hdac2* cKO) and *Hdac1* and *Hdac2* double knockout (cDKO) mice were generated by breeding transgenic mice expressing Cre recombinase under the control of the calcium/calmodulin-dependent kinase II promoter (*CaMKII-Cre93* line) with $Hdac1^{loxP/loxP}$, $Hdac2^{loxP/loxP}$, or $Hdac1^{loxP/loxP}$/$Hdac2^{loxP/loxP}$ mice[23,38]. Previous work has demonstrated that the *CaMKII-Cre93* mice express Cre recombinase at postnatal days 10–14 selectively in forebrain neurons[13]. The $Hdac1^{loxP/loxP}$, $Hdac2^{loxP/loxP}$, and the *CaMKII-Cre93* lines were on a mixed 129/BALBC background and backcrossed to a C57BL/6 line for at least 10 generations. The *Hdac1* cKO, *Hdac2* cKO, and cDKO mice were genotyped using PCR analysis from genomic DNA isolated from tails as previously described[23]. Littermates not carrying the Cre recombinase transgene regardless of loxP alleles were used as control mice in all experiments. Conditional *Mecp2* knockout (*Mecp2* cKO) mice are previously reported[14]. Mice were maintained on a 12 hour light/dark cycle with *ad libitum* access to food and water. Mice were housed 3–5 mice per cage, with the exception of when mice were singly housed for

analyzing the lesion in cDKO mice. All animal protocols were approved by the Institutional Animal Care and Use Committee at The University of Texas Southwestern Medical Center.

Drug injections

All injections were delivered intraperitoneally on naïve male mice. The cDKO mice and control littermates received a once daily injection of either 0.9% saline or fluoxetine (Eli Lilly) at a concentration of 10 mg kg^{-1} in 0.9% saline, during the morning hours of the day (8am–12pm) for 7 or 21 days.

Protein quantification

Brain regions were dissected out and homogenized in a lysis buffer containing 25 mM HEPES, pH 7.9, 150 mM NaCl, 1 mM PMSF, 20 mM NaF, 1 mM DTT, 0.1% NP40, and proteinase inhibitor cocktails (Sigma), and spun down to isolate the lysate. Protein concentrations were determined by Bradford assays and 20 μg of the protein was loaded on 10% SDS-PAGE gels, electrophoresed, transferred to nitrocellulose membranes, then blocked with 5% non-fat milk prior to overnight incubation with primary antibodies. Dilutions of primary antibodies were 1:2000 for both HDAC1 (Abcam, ab19845)[8] and HDAC2 antibodies (Abcam, ab32117)[8], 1:1000 for MeCP2 antibody (Thermofisher, PA1-888)[39], and 1:50,000 for glyceraldehyde-3-phosphate dehydrogenase (GAPDH) antibody (Cell Signaling Technology, 2118S)[8]. The following day membranes were washed, then incubated with peroxidase-labeled anti-rabbit secondary antibody (Vector, P1-1000) at 1:5000 for HDAC1, HDAC2, and MeCP2, and 1:10,000 for GAPDH. Protein bands were detected using enhanced chemiluminescense (ECL) and exposed to film. Immunoreactivity was quantitated by the NIH image J analysis software. HDAC1 or HDAC2 was normalized to GAPDH bands. For HDAC1 and HDAC2 westerns, following the transfer, each membrane was cut below the 50 KDa marker in order to individually probe for either HDAC1 or HDAC2, and GAPDH on the same blot. Separate gels were run for FC, HC, STR, and CBL and all blots were processed in parallel. For western blot following immunoprecipitation, primary antibodies were 1:1000 for MeCP2 (Thermofisher, PA1-888) and 1:6000 for Actin (Abcam, ab6276)[40]. Secondary antibodies were 1:5000 for IRDye® 680RD donkey anti-mouse (LI-COR, 926-68072) and 1:5000 for IRDye® 800CW donkey anti-rabbit (LI-COR, 926-32213). Blots were imaged using a LICOR Odyssey® CLx Imaging System (LI-COR).

Immunohistochemistry

Mice were transcardially perfused with 4% paraformaldehyde (PFA) in 0.1 M phosphate-buffered saline (PBS) and brains were removed from the skull. Following post-fixation in 4% PFA overnight, the brains were cryo-protected in 30% sucrose in 0.1M PBS prior to sectioning on a freezing microtome. The brains were coronally sectioned at 30 μm and subjected to immunohistochemistry. Briefly, free floating sections were incubated overnight in primary antibody solution composed of 3% normal goat serum, and 0.3% Triton X-100 in PBS. Dilutions for the primary antibodies were 1:250 for rabbit anti-HDAC1 (Abcam, ab19845)[8], 1:2000 for rabbit anti-HDAC2 (Abcam, ab32117)[8], 1:1600 for anti-HA (Cell Signaling, 3724S)[41], and 1:200 for anti-GFP (Cell Signaling, 2956S). For HDAC1 staining, the sections were treated in 10 mM citric acid (pH 6) for 15 minutes at 95 °C for antigen

retrieval prior to the primary antibody incubation. Immunoreactivity was visualized by secondary antibodies conjugated with either Alexa Fluor 594 (HDAC1, Invitrogen, A11012)[8] or Alexa Flour 488 (HDAC2, HA, GFP, Invitrogen, A11008)[42]. The sections were incubated at a 1:200 dilution at room temperature for 2 hours, counter-stained with 4′,6-diamidino-2-phenylindole (DAPI), and then mounted on superfrost plus slides in Vectashield mounting media (Vector Laboratories).

Hematoxylin and Eosin (H&E) Staining

H&E staining was carried out as previously described[38]. Briefly, paraffin sections made from formalin fixed tissue were affixed to microscope slides through sequential room temperature and heated air-drying. Dried sections were deparaffinized and stained with hematoxylin, then destained using 70% ethanol. Sections were then stained with eosin, destained, and dehydrated in ascending ethanol solutions. Sections were rinsed in xylene then cover slipped with synthetic mounting media.

TUNEL

Terminal deoxynucleotidyltransferase-mediated UTP end labeling (TUNEL) staining for apoptotic cells was done according to the manufacturer's protocol (Promega DeadEnd Fluorometric TUNEL System, Madison, WI). Apoptotic cells were labeled with fluorescein and the sections were counterstained with propidium iodide.

Vector construction and AAV preparation

A lentiviral vector containing the initial eGFP-SAPAP3 construct was received from the lab of Dr. Guoping Feng. Two AAV vectors were constructed from this plasmid. The eGFP and SAPAP3 were PCR amplified independently and cloned using standard methods into an expression cassette containing the human Synapsin promoter and Growth Hormone polyadenylation signal surrounded by AAV-2 inverted tandem repeats. A Human influenza hemagglutinin (HA) tag was attached to the N-terminus of SAPAP3 during PCR amplification prior to cloning. Primers used were: GFP.EcoRV.R, 5′-ATA TGA TAT CTC ACT TGT ACA GCT CGT CCA TGC CG-3′; GFPSAPAP3.SpeI.F, 5′-ATA TAC TAG TAC CAA TGG TGA GCA AGG GCG AGG AGC-3′; SpeI.HA-SAPAP3F, 5′-ATA TAC TAG TAC CAA TGT ACC CAT ACG ATG TTC CAG ATT ACG CTG GCG GCT CCG GAG GAA GGG GTT ACC ATG G-3′; SAPAP3.EcoRV.R, 5′-ATA TGA TAT CTC ACA GCC TGG TCT GGG CCT CG-3′. pAAV-GFP or pAAV-HA-SAPAP3 were cotransfected with pAAV-DJ and pHelper into HEK-293 cells. 72 hours after transfection, cells were harvested, lysed by freeze-thaw, and incubated with Benzonase (Sigma) at 37 °C. To isolate AAV vector, iodixanol gradient was performed. Cell lysate was transferred to iodixanol gradient in quick-seal centrifugation tube and centrifuged at 48,000 rpm in a Beckman Type 70Ti rotor at 18 °C for 2 hours and 10 minutes. After centrifugation, 40% gradient fraction was collected. Collected fraction was applied onto Amicon Ultra 100K (Millipore), washed with PBS (−) and concentrated. Viral titers were determined by RT-PCR using primers for HGpolyA, and are 1.27×10^{12} GC ml^{-1} for AAV-GFP and 4.9×10^{12} GC ml^{-1} for AAV-SAPAP3.

Adeno-associated virus injection

The adeno-associated virus-green fluorescent protein (AAV-GFP) or adeno-associated virus expressing Cre recombinase tagged with GFP (AAV-GFP-Cre) were obtained from Penn Vector Core; AAV-GFP and AAV-GFP-Cre are AAV1.CMV.PI.EGFP.WPRE.bGH (viral titer of 3.18×10^{13} GC ml^{-1}) and AAV1.CMV.HI.GFP-Cre.SV40 (viral titer of 7.88×10^{12} GC ml^{-1}), respectively. Previous work demonstrated that GFP-tagged Cre recombinase possesses normal enzymatic activity[21,33]. To inject the AAV-GFP, AAV-GFP-Cre or AAV-SAPAP3 in striatum, 3–5 month old naïve *Hdac1*$^{loxP/loxP}$/*Hdac2*$^{loxP/loxP}$ male mice were subjected to stereotaxic surgery as previously described[43]. Briefly, anesthetized animals placed into the stereotaxic frame received 1 μl of AAV-GFP or AAV-GFP-Cre, or 0.5 μl of AAV-SAPAP3 bilaterally with the coordinates relative to Bregma at anteroposterior +1.2 mm, lateral +2.5 mm, and dorsoventral −3.0 mm with a 10° angle. Mice were allowed to recover for three weeks before the commencement of behavioral testing.

RNA extraction and quantitative-RT (qRT) PCR

To determine relative expression of *Hdac1* and *HDAC2* mRNA after stereotaxic AAV injection, we performed qRT-PCR as described previously[21]. Briefly, the animals were sacrificed by rapid decapitation and the brains were sectioned at 14 μm. The dorsal striatum expressing GFP or Cre-GFP was laser microdissected from each section using AS LMD (Leica) system. Eight sections were pooled to extract RNA using PicoPure RNA isolation kit (Arcturus). Each section was 140 μm apart, thus encompassing the majority of the AAV infusion site in the striatum. Conditions for construction of complementary DNA (cDNA) were described earlier[21]. Using cDNA as a template, transcripts for *Hdac1*, *HDAC2*, *Sapap3*, and *Gapdh* were amplified using Power SYBR Green PCR master mix (Applied Biosystems) in a 7500 Real-Time PCR system (Applied Biosystems). The thermal cycling conditions for PCR amplification consisted of 1 cycle of 50 °C for 2 m and 95 °C for 10 m, 40 cycles of 95 °C for 15 s, 60 °C for 60 s, and 1 dissociation cycle of 95 °C for 15 s, 60 °C for 60 s, 95 °C for 15 s, and 60 °C for 15 s. Primers are 5′-agg gca cca aga gga aag tct gtt-3′ and 5′-gca gca aat tgt gag tca tgc gga-3′ for *Hdac1*; 5′-GCG TAC AGT CAA GGA GGC GG-3′ and 5′-GCT TCA TGG GAT GAC CCT GGC-3′ for *Hdac2*; 5′-AGC AGT ACC TTC CCC AGG AT-3′ and 5′-AAA CTG GTC CAG GAG TGT GG-3′ for *Sapap3*; 5′-AGG TCG GTG TGA ACG GAT TTG-3′ and 5′-TGT AGA CCA TGT AGT TGA GGT CA-3′ for *Gapdh*. Primers for *Sapap3* following viral injection with AAV-SAPAP3 are 5′-GTG GAC ACA GCC AGG ATC AAC-3′ and 5′-GCT GCT GCT GGT TAA ACT CTT CGC-3′.

For *Sapap3* expression analysis in *Hdac1* cKO, *Hdac2* cKO, cDKO, and *Mecp2* cKO mice, the following brain regions were dissected: FC, HC, STR, and CBL, and total RNA was extracted using Trizol reagent (Ambion) according to the manufacturer's instructions. Single stranded cDNA was synthesized by treating extracted RNA with random primers and SuperScript Reverse Transcriptase III (Invitrogen). Amplification was performed using Power SYBR Green PCR master mix in a 7500 Real Time PCR detection System (Applied Biosystems).

Immunoprecipitation (IP)

Mouse striata were dissected and homogenized in 120 µl of cold lysis buffer containing 20 mM Tris pH 7.5, 100 mM NaCl, 1 mM EDTA, 1mM PMSF, 0.5% NP40, and protease and phosphatase inhibitor cocktails (1 tablet each of PhosSTOP and cOmplete, Sigma), incubated for 30 minutes at 4 °C on a rotator, then spun down to isolate the lysate. 20 µl of lysate was saved at −20 °C as input material for protein quantification. The remaining lysate was incubated with 880 µl of cold lysis buffer and ~12 µg of anti-HDAC2 (Abcam, ab7029)[44] overnight at 4 °C on a rotator for IP. Recombinant Protein G Agarose beads (Invitrogen) were washed twice with 1X PBS and blocked overnight in 1% BSA at 4 °C on a rotator. The following day, the beads were washed twice with lysis buffer and added to the lysate samples, and rotated for 2 hours at 4 °C. Immunoprecipitates were washed four times with cold lysis buffer, resuspended in 25 µl cold lysis buffer and 20 µl of Laemmli sample buffer (BioRad), boiled and analyzed by western blot.

Chromatin immunoprecipitation (ChIP)

ChIP was performed as previously described[45] with modifications. Briefly, a pool of three dissected mouse striata were homogenized in crosslinking-buffer (0.1 M NaCl, 1 mM EDTA, 0.5 mM EGTA, 25 mM Hepes-KOH, pH 8.0) containing 1% paraformaldehyde. Cross-linking was quenched by adding glycine (final concentration is 125 mM) for 5 minutes after a 10 minute incubation at RT). Cells were then rinsed three times in ice-cold PBS containing complete protease inhibitor cocktail tablets (Roche Diagnostics) and lysed by Buffer I (50 mM Hepes-KOH, pH 7.5, 140 mM NaCl, 1 mM EDTA, pH 8.0, 10 % Glycerol, 0.5 % NP-40, complete protease inhibitor cocktail) for 10 minutes at 4 °C. Nuclei were then pelleted by centrifugation at 2000 g for 10 minutes at 4 °C. The isolated nuclei were rinsed with IP buffer (10 mM Tris-HCl, pH 8.0, 300 mM NaCl, 1 mM EDTA, pH 8.0, 0.5 mM EGTA, pH 8.0, 1% Triton X-100, 0.1% deoxycholic acid (sodium salt) and complete protease inhibitor cocktail). Samples were fragmented by sonication in IP buffer. The sizes of DNA fragments range from 200 bp to 2 kb. Insoluble material was removed by centrifugation at 12,000 g for 10 min at 4 °C. The supernatant was transferred to a new tube and the final volume of the resulting nuclear lysate was adjusted to 1 ml by adding additional IP buffer. 1/20 volume of the ChIP sample (50 µl from 1 ml lysate) was saved as input material. The rest of the lysate was incubated with the indicated antibody (MeCP2 (Millipore, MABE328)[46] or IgG (Millipore, NI04-100UG), 2 µg)[46] overnight at 4 °C for immunoprecipitation.

The next day, 20 µl of pre-rinsed Protein A/G PLUS Agarose (Santa Cruz Biotechnology) was added to each ChIP reaction and further incubated for 2 hours at 4 °C. The beads bound by immune-complexes were pelleted and washed twice with each of the following buffers: low salt buffer (0.1% SDS, 1% Triton X-100, 2 mM EDTA, 20 mM Tris-HCl, pH 8.1, 150 mM NaCl), high salt buffer (0.1% SDS, 1% Triton X-100, 2 mM EDTA, 20 mM Tris-HCl, pH 8.1, 500 mM NaCl), and LiCl buffer (0.25M LiCl, 1% IGEPAL CA630, 1% deoxycholic acid (sodium salt), 1mM EDTA, 10mM Tris, pH 8.1). In each wash, the beads were incubated with wash buffer for 10 minutes at 4 °C. The washed beads were then rinsed once with 1x TE (10 mM Tris-HCl, pH 8.0, 1 mM EDTA). The immunoprecipitated material was eluted from the beads twice by adding 150 µl of elution buffer (10 mM Tris-HCl, pH 8.0, 1

mM EDTA, pH 8.0, 1% SDS) to each ChIP reaction and incubating the sample at 65 °C for 10 min with brief vortexing every 2 minutes. 250 μl of elution buffer was also added to the saved input material (50 μl) and this sample was processed together with the ChIP samples. The eluates were combined and crosslinking was reversed by incubation at 65 °C for ~4–5 hours. To each eluate (300 μl), 5μl of diluted (1:50, 2 mg ml^{-1}) RNaseA (Qiagen) was added and incubated for 1 hour at 37 °C. Then 7 μl of Proteinase K (20 mg ml^{-1}; New England Biolabs) was added and incubated for 2 hours at 50 °C. The immunoprecipitated genomic DNA fragments were extracted with Phenol/Chloroform (Invitrogen). The extracted DNA fragments were then purified using the QIAquick PCR purification kit (Qiagen) and DNA fragments were eluted in 60 μl of 10 mM Tris-HCl, pH 8.5.

ChIP quantitative PCR (QPCR)

For QPCR using ChIP samples, 1 μl of ChIP DNA was used as a direct template and amplification was performed using Power SYBR Green PCR master mix in a 7500 Real Time PCR detection System (Applied Biosystems). Primer sequences for the *Sapap3* P600 region are as follows: 5′-GGG ACT AGT GCG GAG AA-3′ and 5′- TCT TAG GCT CCT GTC CTT AG -3′. For the data analysis, a ΔCt value was obtained by subtracting the ΔCt value of input DNA. A ΔΔCt value was then calculated by subtracting the ΔCt value for IgG. The data are presented as fold enrichment over IgG binding.

Behavioral Overview

For all behavioral testing, experimental animals were male mice, and age matched littermates were used as CTLs. Testing groups for behavioral cohorts were balanced by age and genotype, and randomization of experimental groups was not performed. Mice were naïve prior to the start of the initial behavioral test within each series of experiments. All experiments were conducted during the light cycle and scored by an observer blind to genotypes and group assignments. Mice were habituated to testing facilities 1 hour prior to behavioral assessment. For all experiments, error bars represent either mean ± s.e.m for dot plots or median, 25th and 75th percentile and min and max value of the data set for box-and-whisker plots, and significance was $*P<0.05$. Mice were tested in cohorts for various behavioral tasks. Distinct cohorts of *HDAC1* cKO, *HDAC2* cKO, cDKO, and respective CTL mice were used to assess body weight and brain weight. Distinct cohorts of cDKO mice and CTLs were used to test locomotor activity and open field, and separate cohorts were used to test 6 week and 3 week old mice in each task. A distinct cohort of cDKO and CTL mice was used to score grooming behavior at 6 weeks old, and a separate cohort of cDKO and CTL mice was used to score grooming at 3 weeks old. Separate cohorts of *HDAC1* cKO, *HDAC2* cKO, and respective CTL mice were used to test grooming behavior. A distinct cohort of cDKOs and CTLs was used to test grooming behavior following one week of fluoxetine treatment, and the same cohort was scored for grooming behavior following 3 weeks of fluoxetine treatment. A distinct cohort of $Hdac1^{loxP/loxP}/Hdac2^{loxP/loxP}$ mice was used for stereotaxic injections with AAV-GFP and AAV-GFP-Cre and after recovery this same cohort of mice was tested in multiple behavioral tasks in the following order; locomotor activity, open field, grooming, and rotarod. A distinct cohort of mice was used to assess grooming in *Mecp2* cKO and CTL mice. For rescue experiments using AAV-GFP and AAV-SAPAP3, a distinct cohort of *Mecp2* cKO and CTL mice was used for

stereotaxic injections, and following recovery this same cohort of mice was tested in multiple behavioral tasks in the following order; locomotor activity, grooming, and rotarod.

Locomotor activity

Mice were placed individually in a standard mouse home cage (18 cm × 28 cm) with fresh bedding, and activity was monitored over 2 hours by five horizontal photobeams linked to data acquisition software (Photobeam Activity System, San Diego Instruments, San Diego, CA). Ambulatory activity was measured by counting the number of consecutive beam breaks in 5-minute increments.

Open field

Mice were placed in the periphery of a novel open field environment (44 cm × 44 cm, walls 30 cm high) in a dimly lit room and allowed to explore for 10 min. The animals were monitored from above by a video camera connected to a computer running video tracking software (Ethovision 3.0, Noldus, Leesburg, Virginia) to determine the total time spent in the periphery (5 cm from the walls), center (14 cm × 14 cm), and complete center (34 cm × 34cm). The amount of locomotor activity was also determined and in all experiments was consistent with locomotor activity data using standard mouse home cages. The open field arenas were cleaned between mice.

Rotarod

Each mouse was placed on the rotarod (IITC Life Science), which accelerated from 0 to 45 rpm over the course of 60 seconds. Each session ended when the mouse fell off the rod and the total time spent on the rotarod before falling was measured. The mouse was returned to its original cage for 1 hour. The test was repeated for a total of 8 trials over the course of 2 days (4 trials per day).

Grooming

Grooming behavior was assessed as previously described with modifications[25]. Mice were placed individually into a fresh mouse cage and allowed to move freely for 30 minutes. Test sessions were recorded under red light by a video camera directly in front of the mice located inside the testing room. An observer blind to group and genotype analyzed the video tape and scored self-grooming of any part of the body including the face, head, ears, and full-body grooming. The total amount of time spent grooming (duration) was measured at 10 minute intervals. Continuous grooming for greater than one second was recorded as a grooming bout, and sessions separated by two or more seconds constituted a new bout (modified from Welch et al.).

Statistical analysis

Data are plotted either dot plots with error bars representing mean ± s.e.m, or box-and-whisker plots with interquartile ranges represented as the following: whiskers (error bars) are min and max of data and box is 25th, median, and 75th percentile as calculated in Prism GraphPad software. Statistical differences were calculated in Prism GraphPad software using unpaired, two-tailed *t*-test when comparing two groups, or one-way or two-way

ANOVA with multiple comparisons when appropriate for comparing three or more groups. Tukey, Bonferroni, or Holm-Sidak *post hoc* tests were used following one-way or two-way ANOVA as appropriate. Statistical significance was defined as $*P < 0.05$. For all experiments requiring statistical analysis, the statistical test used, exact P values, sample size (n), t values, ANOVA F values, and degrees of freedom for each experiment is indicated in the figure legend. No statistical methods were used to pre-determine sample sizes, however sample sizes were estimated based on similar experiments reported in previous publications from our lab[8,39,43,47]. Data distribution was assumed to be normal with similar variance between groups, however this was not formally tested. The Grubbs test was used when appropriate to identify and remove significant outliers.

A supplementary methods checklist is available online.

Supplementary Material

Refer to Web version on PubMed Central for supplementary material.

Acknowledgments

This work was supported by National Institute of Health grant MH081060 (LMM) and MH66198 (ETK). The authors thank E. Olson (UT Southwestern Medical Center) for generously providing *Hdac1*$^{loxP/loxP}$/*Hdac2*$^{loxP/loxP}$, *Hdac1*$^{loxP/loxP}$, and *Hdac2*$^{loxP/loxP}$ mice, J. Richardson for performing the necropsy of the mice, and G. Feng (Duke University Medical Center) for the initial vector construct of *Sapap3*. The authors are grateful to E. Olson, R. Bassel-Duby, W. Xu, and TK. Kim for helpful comments and suggestions. We also thank Brent Trauterman for his excellent technical assistance. L. Monteggia holds the Ginny and John Eulich Professorship in Autism Spectrum Disorders at UT Southwestern.

References

1. Haberland M, Montgomery RL, Olson EN. The many roles of histone deacetylases in development and physiology: implications for disease and therapy. Nature reviews Genetics. 2009; 10:32–42. DOI: 10.1038/nrg2485
2. Levenson JM, et al. Regulation of histone acetylation during memory formation in the hippocampus. The Journal of biological chemistry. 2004; 279:40545–40559. DOI: 10.1074/jbc.M402229200 [PubMed: 15273246]
3. Fischer A, Sananbenesi F, Wang X, Dobbin M, Tsai LH. Recovery of learning and memory is associated with chromatin remodelling. Nature. 2007; 447:178–182. DOI: 10.1038/nature05772 [PubMed: 17468743]
4. Vecsey CG, et al. Histone deacetylase inhibitors enhance memory and synaptic plasticity via CREB:CBP-dependent transcriptional activation. The Journal of neuroscience: the official journal of the Society for Neuroscience. 2007; 27:6128–6140. DOI: 10.1523/JNEUROSCI.0296-07.2007 [PubMed: 17553985]
5. Barrett RM, Wood MA. Beyond transcription factors: the role of chromatin modifying enzymes in regulating transcription required for memory. Learn Mem. 2008; 15:460–467. DOI: 10.1101/lm.917508 [PubMed: 18583646]
6. Morris MJ, Karra AS, Monteggia LM. Histone deacetylases govern cellular mechanisms underlying behavioral and synaptic plasticity in the developing and adult brain. Behav Pharmacol. 2010; 21:409–419. DOI: 10.1097/FBP.0b013e32833c20c0 [PubMed: 20555253]
7. Guan JS, et al. HDAC2 negatively regulates memory formation and synaptic plasticity. Nature. 2009; 459:55–60. DOI: 10.1038/nature07925 [PubMed: 19424149]
8. Morris MJ, Mahgoub M, Na ES, Pranav H, Monteggia LM. Loss of histone deacetylase 2 improves working memory and accelerates extinction learning. The Journal of neuroscience: the official

journal of the Society for Neuroscience. 2013; 33:6401–6411. DOI: 10.1523/JNEUROSCI.1001-12.2013 [PubMed: 23575838]

9. Shahbazian MD, Grunstein M. Functions of site-specific histone acetylation and deacetylation. Annu Rev Biochem. 2007; 76:75–100. DOI: 10.1146/annurev.biochem.76.052705.162114 [PubMed: 17362198]
10. Jones PL, et al. Methylated DNA and MeCP2 recruit histone deacetylase to repress transcription. Nature genetics. 1998; 19:187–191. DOI: 10.1038/561 [PubMed: 9620779]
11. Nan X, et al. Transcriptional repression by the methyl-CpG-binding protein MeCP2 involves a histone deacetylase complex. Nature. 1998; 393:386–389. DOI: 10.1038/30764 [PubMed: 9620804]
12. Guy J, Hendrich B, Holmes M, Martin JE, Bird A. A mouse Mecp2-null mutation causes neurological symptoms that mimic Rett syndrome. Nature genetics. 2001; 27:322–326. DOI: 10.1038/85899 [PubMed: 11242117]
13. Chen RZ, Akbarian S, Tudor M, Jaenisch R. Deficiency of methyl-CpG binding protein-2 in CNS neurons results in a Rett-like phenotype in mice. Nature genetics. 2001; 27:327–331. DOI: 10.1038/85906 [PubMed: 11242118]
14. Gemelli T, et al. Postnatal loss of methyl-CpG binding protein 2 in the forebrain is sufficient to mediate behavioral aspects of Rett syndrome in mice. Biological psychiatry. 2006; 59:468–476. DOI: 10.1016/j.biopsych.2005.07.025 [PubMed: 16199017]
15. Nelson ED, Kavalali ET, Monteggia LM. MeCP2-dependent transcriptional repression regulates excitatory neurotransmission. Curr Biol. 2006; 16:710–716. DOI: 10.1016/j.cub.2006.02.062 [PubMed: 16581518]
16. Chao HT, Zoghbi HY, Rosenmund C. MeCP2 controls excitatory synaptic strength by regulating glutamatergic synapse number. Neuron. 2007; 56:58–65. DOI: 10.1016/j.neuron.2007.08.018 [PubMed: 17920015]
17. Amir RE, et al. Rett syndrome is caused by mutations in X-linked MECP2, encoding methyl-CpG-binding protein 2. Nature genetics. 1999; 23:185–188. DOI: 10.1038/13810 [PubMed: 10508514]
18. Moretti P, Zoghbi HY. MeCP2 dysfunction in Rett syndrome and related disorders. Curr Opin Genet Dev. 2006; 16:276–281. DOI: 10.1016/j.gde.2006.04.009 [PubMed: 16647848]
19. Hagberg B, Aicardi J, Dias K, Ramos O. A progressive syndrome of autism, dementia, ataxia, and loss of purposeful hand use in girls: Rett's syndrome: report of 35 cases. Ann Neurol. 1983; 14:471–479. DOI: 10.1002/ana.410140412 [PubMed: 6638958]
20. Zoghbi H. Genetic aspects of Rett syndrome. J Child Neurol. 1988; 3(Suppl):S76–78. [PubMed: 3058791]
21. Adachi M, Autry AE, Covington HE 3rd, Monteggia LM. MeCP2-mediated transcription repression in the basolateral amygdala may underlie heightened anxiety in a mouse model of Rett syndrome. The Journal of neuroscience: the official journal of the Society for Neuroscience. 2009; 29:4218–4227. DOI: 10.1523/JNEUROSCI.4225-08.2009 [PubMed: 19339616]
22. Chao HT, et al. Dysfunction in GABA signalling mediates autism-like stereotypies and Rett syndrome phenotypes. Nature. 2010; 468:263–269. DOI: 10.1038/nature09582 [PubMed: 21068835]
23. Montgomery RL, et al. Histone deacetylases 1 and 2 redundantly regulate cardiac morphogenesis, growth, and contractility. Genes & development. 2007; 21:1790–1802. DOI: 10.1101/gad.1563807 [PubMed: 17639084]
24. Fan G, et al. DNA hypomethylation perturbs the function and survival of CNS neurons in postnatal animals. The Journal of neuroscience: the official journal of the Society for Neuroscience. 2001; 21:788–797. [PubMed: 11157065]
25. Welch JM, et al. Cortico-striatal synaptic defects and OCD-like behaviours in Sapap3-mutant mice. Nature. 2007; 448:894–900. DOI: 10.1038/nature06104 [PubMed: 17713528]
26. Shmelkov SV, et al. Slitrk5 deficiency impairs corticostriatal circuitry and leads to obsessive-compulsive-like behaviors in mice. Nat Med. 2010; 16:598–602. 591p following 602. DOI: 10.1038/nm.2125 [PubMed: 20418887]
27. McDougle CJ. Update on pharmacologic management of OCD: agents and augmentation. J Clin Psychiatry. 1997; 58(Suppl 12):11–17.

28. Rapoport JL, Inoff-Germain G. Treatment of obsessive-compulsive disorder in children and adolescents. J Child Psychol Psychiatry. 2000; 41:419–431. [PubMed: 10836672]
29. Vythilingum B, Cartwright C, Hollander E. Pharmacotherapy of obsessive-compulsive disorder: experience with the selective serotonin reuptake inhibitors. Int Clin Psychopharmacol. 2000; 15(Suppl 2):S7–13.
30. Charney, DS.; Nestler, EJ.; Sklar, P.; Buxbaum, JD. Neurobiology of mental illness. Oxford University Press; 2013.
31. Bienvenu OJ, et al. Sapap3 and pathological grooming in humans: Results from the OCD collaborative genetics study. American journal of medical genetics. Part B, Neuropsychiatric genetics: the official publication of the International Society of Psychiatric Genetics. 2009; 150B: 710–720. DOI: 10.1002/ajmg.b.30897
32. Zuchner S, et al. Multiple rare SAPAP3 missense variants in trichotillomania and OCD. Molecular psychiatry. 2009; 14:6–9. DOI: 10.1038/mp.2008.83 [PubMed: 19096451]
33. Berton O, et al. Essential role of BDNF in the mesolimbic dopamine pathway in social defeat stress. Science. 2006; 311:864–868. DOI: 10.1126/science.1120972 [PubMed: 16469931]
34. Grunstein M. Histone acetylation in chromatin structure and transcription. Nature. 1997; 389:349–352. DOI: 10.1038/38664 [PubMed: 9311776]
35. Chahrour M, et al. MeCP2, a key contributor to neurological disease, activates and represses transcription. Science. 2008; 320:1224–1229. DOI: 10.1126/science.1153252 [PubMed: 18511691]
36. Yasui DH, et al. Integrated epigenomic analyses of neuronal MeCP2 reveal a role for long-range interaction with active genes. Proceedings of the National Academy of Sciences of the United States of America. 2007; 104:19416–19421. DOI: 10.1073/pnas.0707442104 [PubMed: 18042715]
37. Kent WJ, et al. The human genome browser at UCSC. Genome Res. 2002; 12:996–1006. Article published online before print in May 2002. DOI: 10.1101/gr.229102. [PubMed: 12045153]
38. Montgomery RL, Hsieh J, Barbosa AC, Richardson JA, Olson EN. Histone deacetylases 1 and 2 control the progression of neural precursors to neurons during brain development. Proceedings of the National Academy of Sciences of the United States of America. 2009; 106:7876–7881. DOI: 10.1073/pnas.0902750106 [PubMed: 19380719]
39. Na ES, et al. A mouse model for MeCP2 duplication syndrome: MeCP2 overexpression impairs learning and memory and synaptic transmission. The Journal of neuroscience: the official journal of the Society for Neuroscience. 2012; 32:3109–3117. DOI: 10.1523/JNEUROSCI.6000-11.2012 [PubMed: 22378884]
40. Adeosun SO, et al. Cognitive deficits and disruption of neurogenesis in a mouse model of apolipoprotein E4 domain interaction. The Journal of biological chemistry. 2014; 289:2946–2959. DOI: 10.1074/jbc.M113.497909 [PubMed: 24324264]
41. Liu X, et al. Interleukin 1 type 1 receptor restore: a genetic mouse model for studying interleukin 1 receptor-mediated effects in specific cell types. The Journal of neuroscience: the official journal of the Society for Neuroscience. 2015; 35:2860–2870. DOI: 10.1523/JNEUROSCI.3199-14.2015 [PubMed: 25698726]
42. Fremont R, Tewari A, Khodakhah K. Aberrant Purkinje cell activity is the cause of dystonia in a shRNA-based mouse model of Rapid Onset Dystonia-Parkinsonism. Neurobiol Dis. 2015; 82:200–212. DOI: 10.1016/j.nbd.2015.06.004 [PubMed: 26093171]
43. Adachi M, Barrot M, Autry AE, Theobald D, Monteggia LM. Selective loss of brain-derived neurotrophic factor in the dentate gyrus attenuates antidepressant efficacy. Biological psychiatry. 2008; 63:642–649. DOI: 10.1016/j.biopsych.2007.09.019 [PubMed: 17981266]
44. Potts RC, et al. CHD5, a brain-specific paralog of Mi2 chromatin remodeling enzymes, regulates expression of neuronal genes. PLoS One. 2011; 6:e24515. [PubMed: 21931736]
45. Flavell SW, et al. Genome-wide analysis of MEF2 transcriptional program reveals synaptic target genes and neuronal activity-dependent polyadenylation site selection. Neuron. 2008; 60:1022–1038. DOI: 10.1016/j.neuron.2008.11.029 [PubMed: 19109909]
46. Li W, Calfa G, Larimore J, Pozzo-Miller L. Activity-dependent BDNF release and TRPC signaling is impaired in hippocampal neurons of Mecp2 mutant mice. Proceedings of the National Academy

of Sciences of the United States of America. 2012; 109:17087–17092. DOI: 10.1073/pnas.1205271109 [PubMed: 23027959]

47. Autry AE, et al. NMDA receptor blockade at rest triggers rapid behavioural antidepressant responses. Nature. 2011; 475:91–95. DOI: 10.1038/nature10130 [PubMed: 21677641]

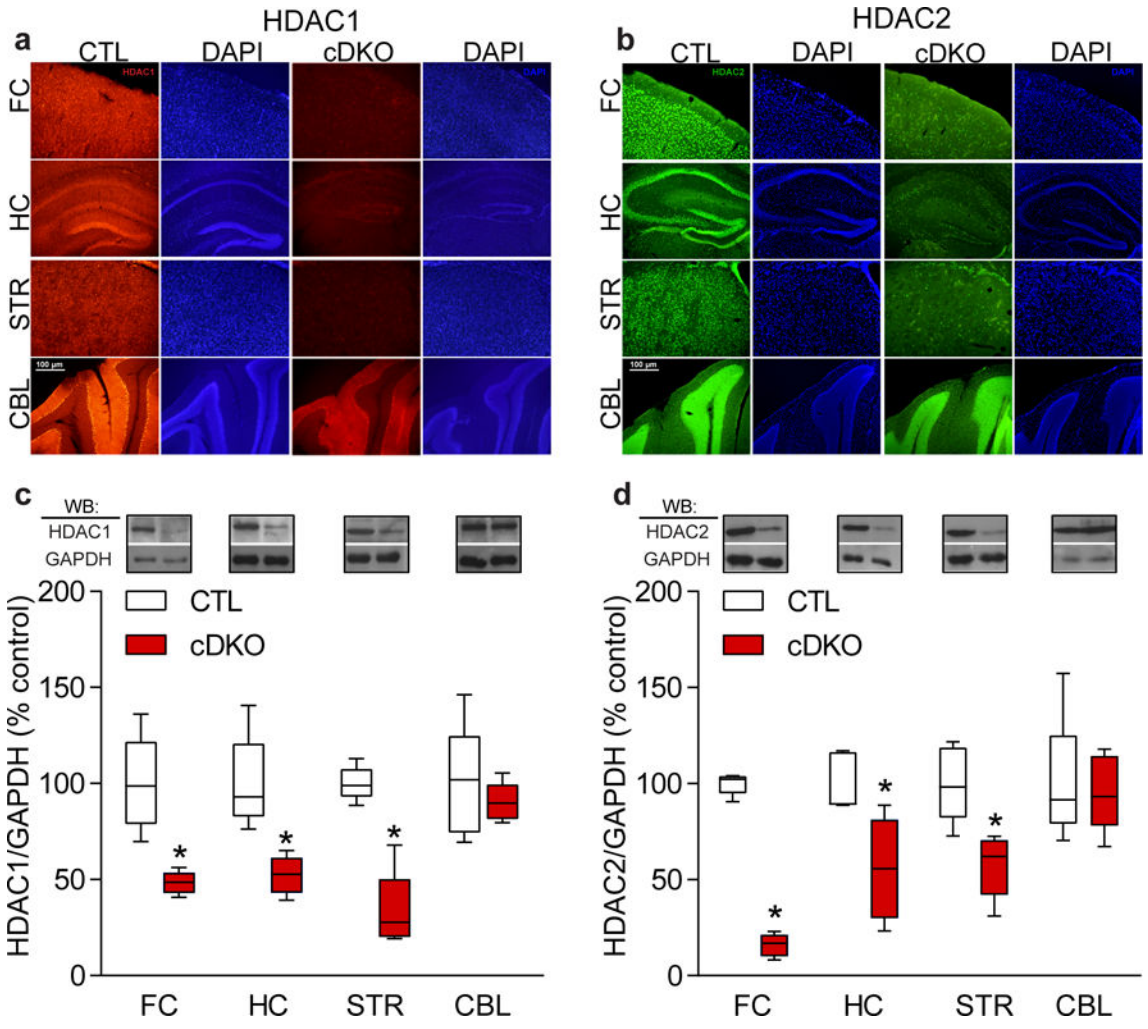

Figure 1.

Characterization of conditional *HDAC1* and *HDAC2* double knockout (cDKO) mice. Fluorescent immunohistochemistry confirmed a selective loss of HDAC1 (**a**) and HDAC2 (**b**) in forebrain regions (frontal cortex (FC), striatum (STR), and hippocampus (HC)) but not in cerebellum (CBL) of cDKO mice. Images were captured using an Olympus BX51 epifluorescence microscope and Olympus DP70 software. Scale bar represents 100 μm. Presented are representative images from a cohort of cDKO mice and respective CTLs, and results were replicated in a second cohort of mice. (**c,d**) Western blot analysis confirmed over 50% reduction of HDAC1 (normalized to GAPDH) (**c**) and HDAC2 (normalized to GAPDH) (**d**) in forebrain regions of cDKO mice with no alterations in CBL. Full length blots are presented in Supplementary Fig. 8 (n=5 mice per group for HDAC1; two-tailed t-test; $t_{(8)}$ = 4.577; P = 0.0018 for FC CTL versus cDKO; $t_{(8)}$ = 4.408; P = 0.0037 for HC CTL versus cDKO; $t_{(8)}$ = 6.832; P = 0.0001 for STR CTL versus cDKO; $t_{(8)}$ = 0.6912; P = 0.5090 for CBL CTL versus cDKO; n=5 mice per group for HDAC2; two-tailed t-test; $t_{(8)}$ = 23.06; P < 0.0001 for FC CTL versus cDKO; $t_{(8)}$ = 3.247; P = 0.0118 for HC CTL versus cDKO; $t_{(8)}$ = 3.715; P = 0.0059 for STR CTL versus cDKO; $t_{(8)}$ = 0.8062; P = 0.2536 for CBL CTL

versus cDKO). Data are shown as median, 25th and 75th percentile, and min and max value (**c**–**d**). *$P < 0.05$.

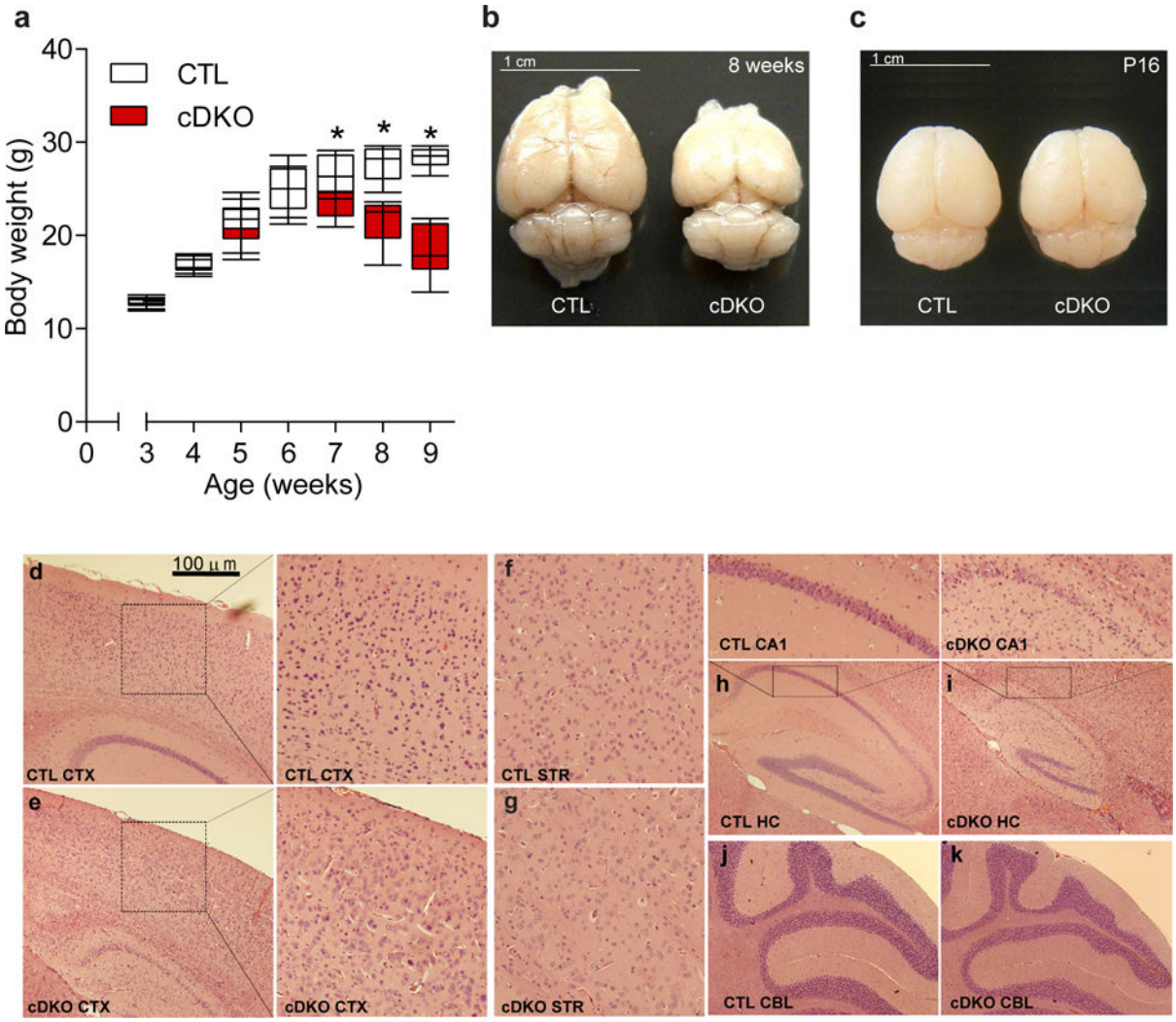

Figure 2.

Conditional forebrain deletion of *HDAC1* and *HDAC2* leads to premature death. (**a**) cDKO mice significantly lose body weight after 6 weeks of age (n=6 mice per group; two-tailed t-test; $t_{(10)}$ = 0.1132; P = 0.9121 for 3 weeks CTL versus cDKO; two-tailed t-test; $t_{(10)}$ = 0.1838; P = 0.8579 for 4 weeks CTL versus cDKO; two-tailed t-test; $t_{(10)}$ = 0.1854; P = 0.8566 for 5 weeks CTL versus cDKO; two-tailed t-test; $t_{(10)}$ = 0.1417; P = 0.8901 for 6 weeks CTL versus cDKO; two-tailed t-test; $t_{(10)}$ = 2.278; P = 0.0460 for 7 weeks CTL versus cDKO; two-tailed t-test; $t_{(10)}$ = 4.72; P = 0.0008 for 8 weeks CTL versus cDKO; two-tailed t-test; $t_{(10)}$ = 7.922; P < 0.0001 for 9 weeks CTL versus cDKO). (**b,c**) Representative pictures indicating forebrain volume was smaller in cDKO than in CTLs in 8 week old mice (**b**) with no changes observed at P16 (**c**). Images were captured using a Nikon DSLR camera. Scale bar represents 1 cm and results were replicated in > 30 cohorts of mice at 8 weeks of age, and in two cohorts of mice at P16. (**d**–**k**) Representative images of Hematoxylin and Eosin (H&E) staining. cDKO mice (**e and enlarged**) have disrupted cortical lamination compared to CTLs (**d and enlarged**). Striatal patterns of cDKO mice (**g**) are indistinguishable from CTLs (**f**). Overall hippocampal size was dramatically smaller and

granule cell layers of CA1 were disrupted in cDKO (**i and enlarged**), compared to CTLs (**h and enlarged**). No histological differences were observed in the cerebellum (CBL) between cDKO **(k)** and CTLs **(j)**. Results were replicated in two additional cohorts of mice. Images were captured using an Olympus BX51 brightfield microscope and Olympus DP70 software. Scale bar represents 100 μm and enlarged images were taken at 40× magnification. Data are shown as median, 25th and 75th percentile, and min and max value (**a**). $*P < 0.05$.

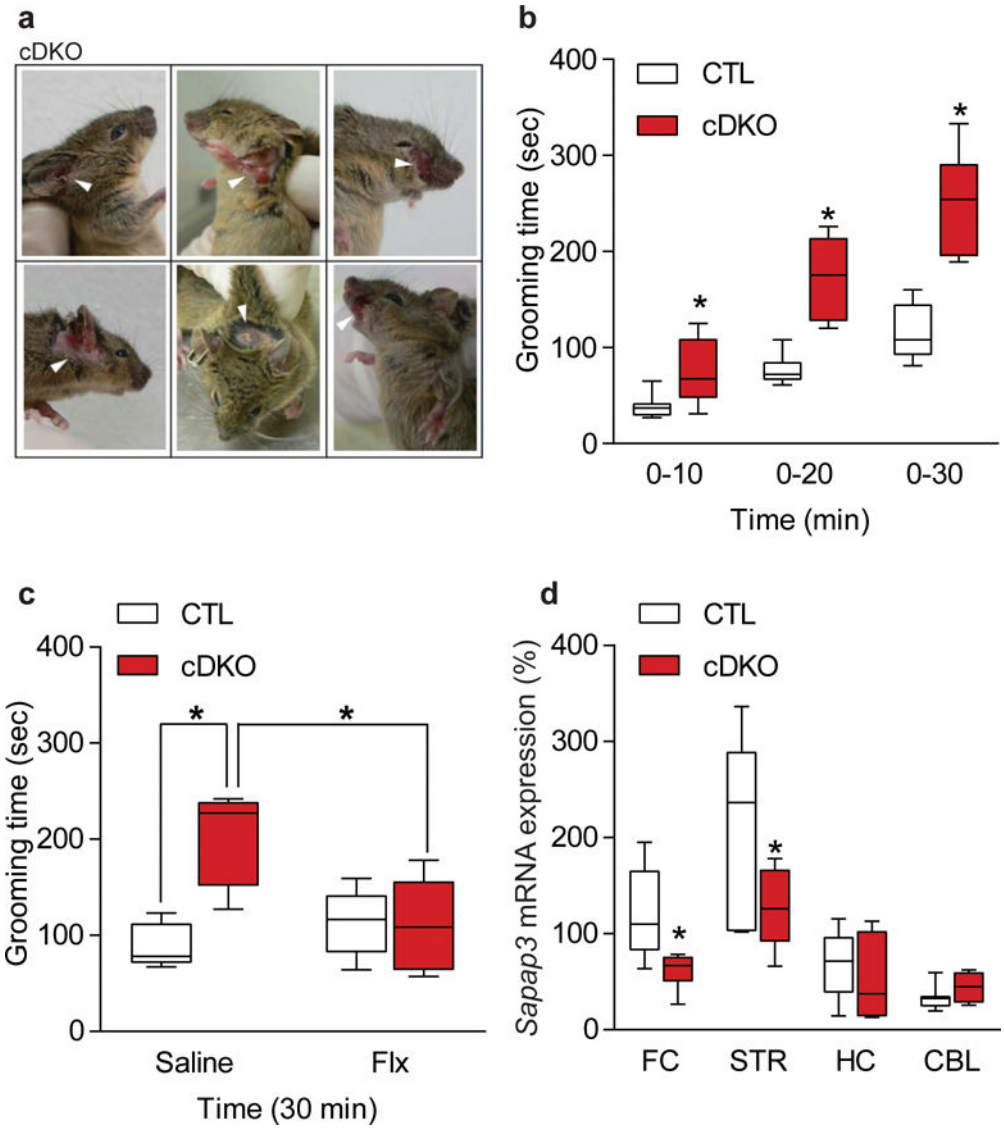

Figure 3.

HDAC1 and *HDAC2* cDKO mice have increased grooming behavior and dysregulation of SAPAP3. (**a**) Representative images of the facial lesion which occurs in every cDKO mouse at approximately 7 weeks of age. Results were replicated in every DKO mouse generated in this study. Images were captured using a Nikon DSLR camera. (**b**) Grooming behavior was assessed by quantifying the total time spent grooming over a 30 minute period. cDKO mice spend significantly more time grooming at 6 weeks of age compared to littermate CTL mice (CTL n=7; cDKO n=6; two-tailed t-test; $t_{(11)} = 2.556$; $P = 0.0267$ for 0–10 min CTL versus cDKO; $t_{(11)} = 5.129$; $P = 0.0003$ for 0–20 min CTL versus cDKO; $t_{(11)} = 5.787$; $P = 0.0001$ for 0–30 min CTL versus cDKO). (**c**) Fluoxetine (Flx) administration for 21 days attenuated the grooming phenotype in cDKOs to levels comparable to CTLs (CTL Saline n=5; CTL Flx n=6; cDKO Saline n=4; cDKO Flx n=6; two-way ANOVA $F_{(1,17)} = 11.1$, $P = 0.0039$ for treatment; Tukey's *post hoc* analysis for CTL Saline versus cDKO Saline $P = 0.0024$, cDKO Saline versus cDKO Flx $P = 0.0119$). (**d**) Quantitative-RT (qRT) PCR analysis showed that

Sapap3 mRNA levels were significantly down-regulated in the frontal cortex (FC) and striatum (STR) of conditional cDKO mice compared to CTLs, with no change in the hippocampus (HC) and cerebellum (CBL) (FC CTL n=7, cDKO n=6; STR CTL n=6, cDKO=7; HC CTL n=8, cDKO n=7; CBL CTL n=7, cDKO=4; two-tailed t-test; $t_{(11)}$ = 2.769; P = 0.0183 for FC CTL versus cDKO; $t_{(11)}$ = 2.278; P = 0.0437 for STR CTL versus cDKO; $t_{(13)}$ = 0.9407; P = 0.3640 for HC CTL versus cDKO; $t_{(9)}$ = 1.181; P = 0.2677 for CBL CTL versus cDKO). Data are shown as median, 25th and 75th percentile, and min and max value (**b**–**d**). *P < 0.05.

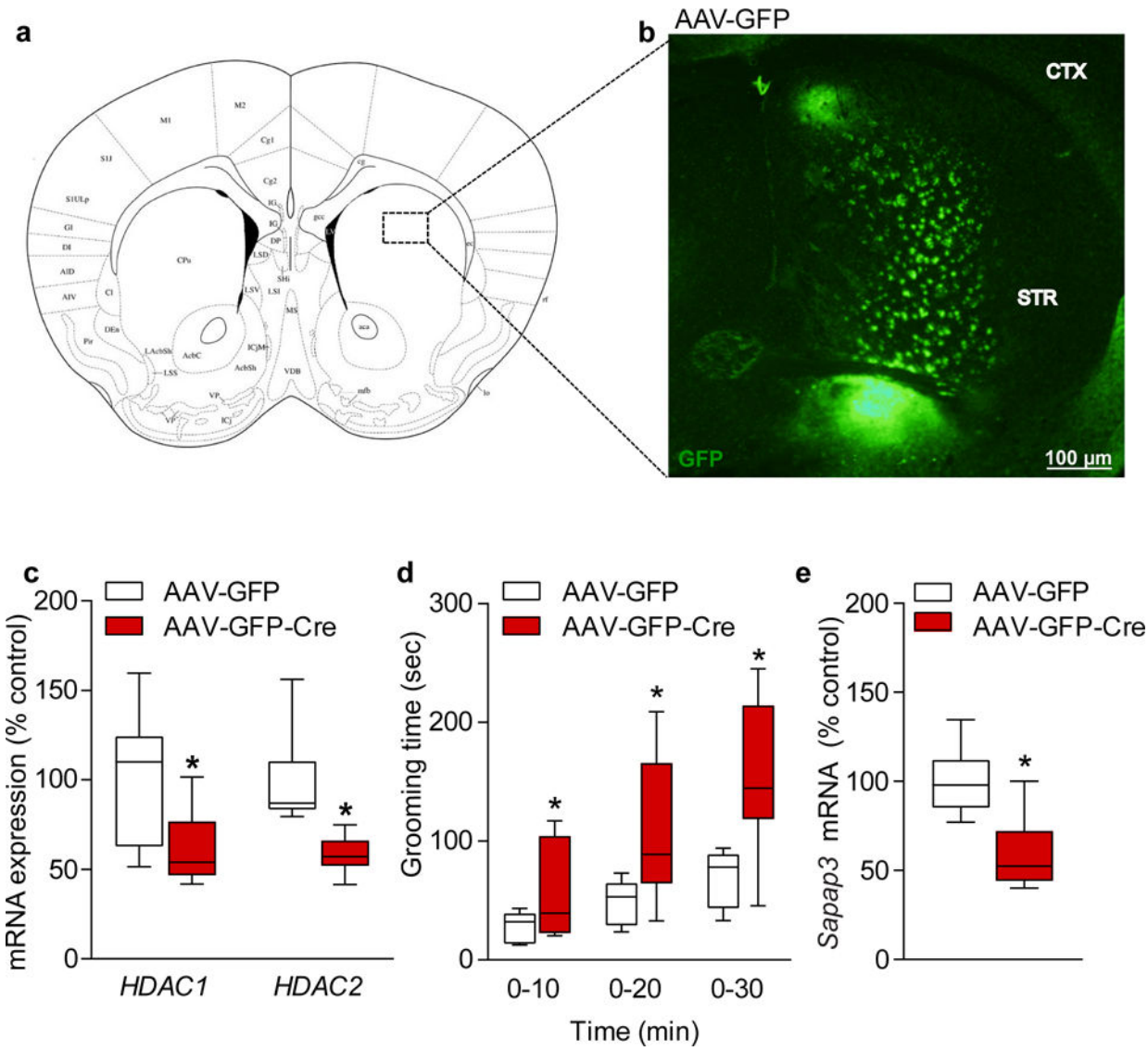

Figure 4.

Striatal specific deletion of *HDAC1* and *HDAC2* recapitulates the excessive grooming phenotype. (**a**) Representative diagram of the approximate virus injection site in the dorsal striatum of $Hdac1^{loxP/loxP}/Hdac2^{loxP/loxP}$ mice. (**b**) Striatal sections containing GFP epifluorescence were laser microdissected and subjected to quantitative-RT (qRT) PCR for quantitation of *Hdac1* and *Hdac2* mRNA levels. Presented is a representative coronal section indicating the GFP infected neurons at the injection site. Images were captured using an Olympus BX51 epifluorescence microscope and Olympus DP70 software. Results were replicated in seven additional mice. Scale bar represents 100 µm. (**c**) Quantitative-RT (qRT) PCR confirmed a significant knockdown of approximately 50% of both of *Hdac1* and *Hdac2* mRNA levels in the striatum of $Hdac1^{loxP/loxP}/Hdac2^{loxP/loxP}$ mice which received AAV-GFP-Cre, in comparison to mice which received AAV-GFP (HDAC1 AAV-GFP n=7; AAV-GFP-Cre n=6; two-tailed t-test; $t_{(11)} = 2.211$; $P = 0.0491$ for AAV-GFP versus AAV-GFP-Cre; HDAC2 AAV-GFP n=7; AAV-GFP-Cre n=8; two-tailed t-test; $t_{(13)} = 4.084$; $P = 0.0013$

for AAV-GFP versus AAV-GFP-Cre). (**d**) *Hdac1*$^{loxP/loxP}$/*Hdac2*$^{loxP/loxP}$ mice which received AAV-GFP-Cre spent significantly more time grooming compared to *Hdac1*$^{loxP/loxP}$/*Hdac2*$^{loxP/loxP}$ mice injected with AAV-GFP, recapitulating a similar phenotype observed in the cDKO mice (AAV-GFP n=9; AAV-GFP-Cre n=8; two-tailed t-test; $t_{(15)} = 2.134$; $P = 0.0497$ for 0–10 min AAV-GFP versus AAV-GFP-Cre; $t_{(15)} = 2.863$; $P = 0.0119$ for 0–20 min AAV-GFP versus AAV-GFP-Cre; $t_{(15)} = 3.709$; $P = 0.0021$ for 0–30 min AAV-GFP versus AAV-GFP-Cre). (**e**) Striatal mRNA expression of *Sapap3* in the *Hdac1*$^{loxP/loxP}$/*Hdac2*$^{loxP/loxP}$ mice injected with AAV-GFP-Cre was significantly reduced compared to those with AAV-GFP (AAV-GFP n=6; AAV-GFP-Cre n=6; two-tailed t-test; $t_{(10)} = 3.425$; $P = 0.0065$ for AAV-GFP versus AAV-GFP-Cre). Data are shown as median, 25th and 75th percentile, and min and max value (**c**–**e**). *$P < 0.05$.

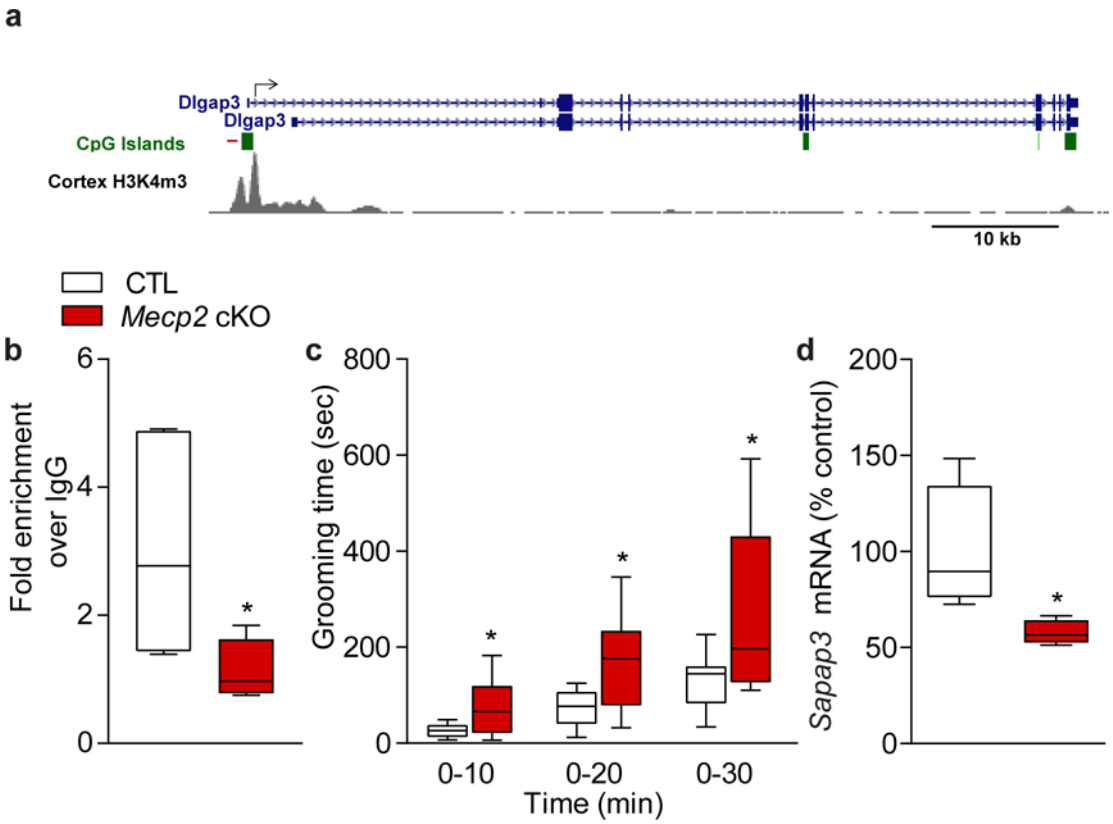

Figure 5.

Loss of *Mecp2* leads to excessive grooming and dysregulation of SAPAP3. (**a**) The *Sapap3* (*Dlgap3*) promoter region showing the location of ChIP QPCR primers (red line) relative to the transcription start site (arrow) and the adjacent CpG island (green rectangle). The H3K4me3 promoter mark is based on mouse cortex ChIP-seq data from the LICR Histone track of the University of California Santa Cruz genome browser (http://genome.ucsc.edu), NCBI37/mm9 mouse genome build[37]. (**b**) MeCP2 binds to the promoter region of *Sapap3*. ChIP with antibody to MeCP2 shows that it binds to the promoter region of *Sapap3*. QPCR data are normalized to input and plotted as fold enrichment over IgG (n=5 for all groups; two-tailed t-test; $t_{(8)} = 2.404$; $P = 0.0429$ for CTL versus cKO). (**c**) Conditional *Mecp2* cKO mice (cKO) spend significantly more time grooming compared to littermate CTL mice (CTL n=15; *Mecp2* cKO n=12; two-tailed t-test; $t_{(25)} = 3.133$; $P = 0.0044$ for 0–10 min CTL versus *Mecp2* cKO; $t_{(25)} = 3.62$; $P = 0.0013$ for 0–20 min CTL versus *Mecp2* cKO; $t_{(25)} = 3.036$; $P = 0.0055$ for 0–30 min CTL versus *Mecp2* cKO). (**d**) *Sapap3* mRNA expression in the striatum of *Mecp2* cKO mice is significantly reduced compared to CTLs (n=4 mice per group; two-tailed t-test; $t_{(6)} = 2.487$; $P = 0.0474$ for CTL versus *Mecp2* cKO). Data are shown as median, 25th and 75th percentile, and min and max value (**b**–**d**). *$P < 0.05$.

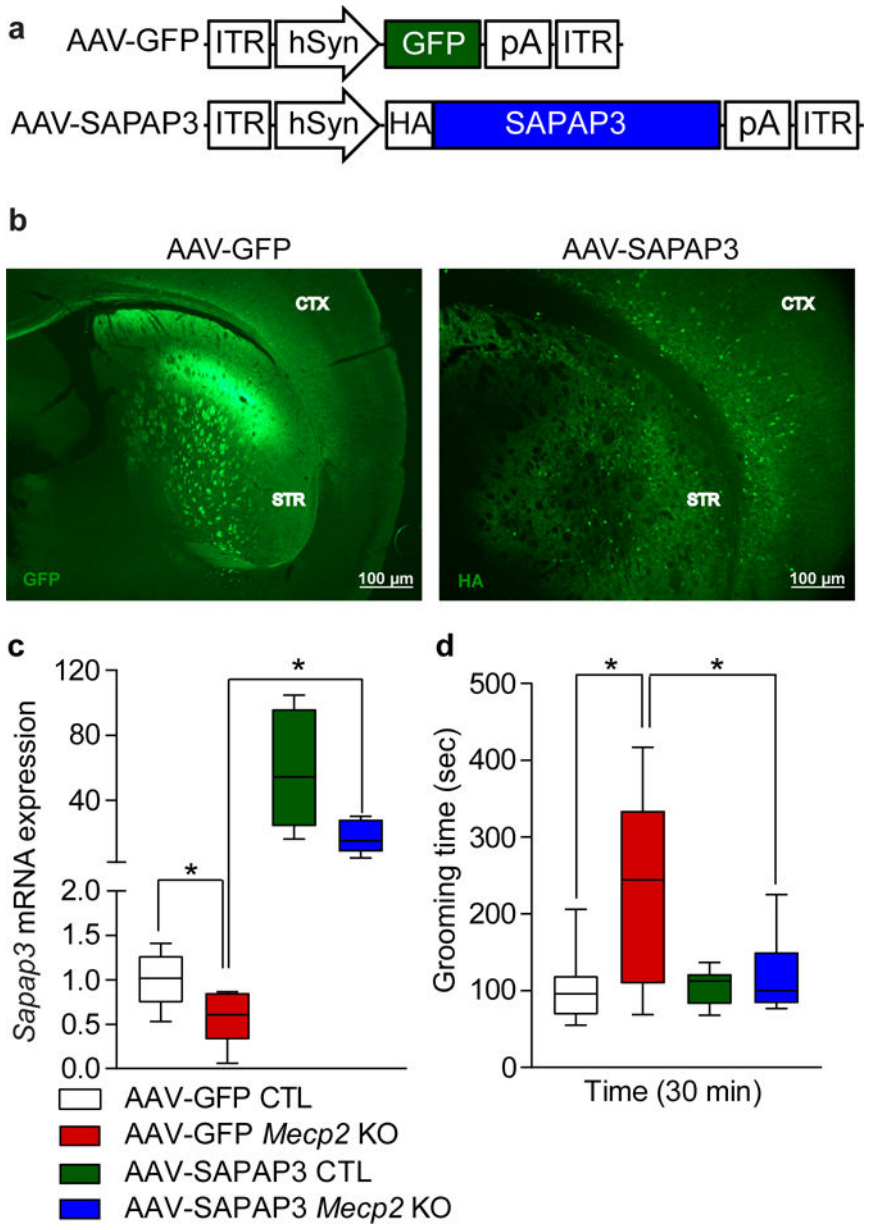

Figure 6.

Restoring MeCP2 in the striatum rescues grooming behavior in *Mecp2* cKO mice. (**a**) Diagram representing the map of the AAV-GFP and AAV-SAPAP3 constructs. (**b**) Representative images of approximate virus injection site in the dorsal striatum for Sapap3 rescue experiments. Coronal sections were immunostained using anti-GFP (left) and anti-HA (right) to visualize infectivity. Results were replicated in a second cohort of mice. Images were captured on a Nikon ECLIPSE 80i Upright microscope using NIS-element software. Scale bar represents 100 µm. (**c**) Striatal mRNA expression of *Sapap3* in *Mecp2* cKO animals injected with AAV-GFP is significantly reduced by approximately 50% compared to CTL mice. *Mecp2* cKO mice injected with AAV-SAPAP3 show rescued expression of *Sapap3* compared to *Mecp2* cKO mice injected with AAV-GFP virus (AAV-GFP CTL n=9; AAV-GFP *Mecp2* cKO n=6; AAV-SAPAP3 CTL n=8; AAV-SAPAP3 *Mecp2*

cKO n=5; two-way ANOVA $F_{(1,24)}$ = 7.752, P = 0.0103 for interaction; Holm-Sidak *post hoc* analysis for multiple comparisons for AAV-GFP CTL versus AAV-GFP *Mecp2* cKO P = 0.0162, AAV-GFP *Mecp2* cKO versus AAV-SAPAP3 *Mecp2* cKO P = 0.0027). (**d**) *Mecp2* cKO mice injected with AAV-GFP spend significantly more time grooming compared to CTL mice injected with AAV-GFP. Excessive grooming is alleviated in *Mecp2* cKO mice injected with AAV-SAPAP3 to levels comparable to AAV-GFP CTLs (AAV-GFP CTL n=10; AAV-GFP *Mecp2* cKO n=8; AAV-SAPAP3 CTL n=10; AAV-SAPAP3 *Mecp2* cKO n=7; two-way ANOVA $F_{(1,31)}$ = 0.0190, P = 0.0190 for interaction; Tukey's *post hoc* analysis for AAV-GFP CTL versus AAV-GFP *Mecp2* cKO P = 0.0017, AAV-GFP *Mecp2* cKO versus AAV-SAPAP3 *Mecp2* cKO P = 0.0158). Data are shown as median, 25th and 75th percentile, and min and max value (**c**–**d**). *P < 0.05.